Journal of Solid State Chemistry 184 (2011) 690–697

Contents lists available at ScienceDirect

Journal of Solid State Chemistry

journal homepage: www.elsevier.com/locate/jssc

Assemblies based on the directing effect of non-classical W_{18} anionic clusters and the rod-like trans-1,2-di-(4-pyridyl)-ethylen (bpe)

Zhangang Han [a,*], Yanna Wang [a], Xuejun Song [b], Jiao Huang [a], Xueliang Zhai [a,*]

[a] College of Chemistry & Material Science, Hebei Normal University, Shijiazhuang, Hebei 050016, China
[b] College of Physics Science and Information Engineering, Hebei Normal University, Shijiazhuang, Hebei 050016, China

ARTICLE INFO

Article history:
Received 2 September 2010
Received in revised form
15 January 2011
Accepted 31 January 2011
Available online 4 February 2011

Keywords:
Supramolecular assembly
Polyoxometalate
Conjugated system
Hydrogen bond
π-stacking

ABSTRACT

Two polyoxometalate (POM) supramolecular assemblies based on W_{18} clusters and the rigid organic trans-1,2-di-(4-pyridyl)-ethylen (bpe) have been synthesized and fully characterized, namely $(H_2bpe)3.5H_2[SbW_{18}O_{60}]\cdot 5H_2O$ (**1**), and $(H_2bpe)5[Ni_4(AsW_9O_{34})_2(H_2O)_2]\cdot 3H2O$ (**2**). Compounds **1–2** are formed from organic bpe cations and different polytungstate anions: pseudo-Dawson-type $[SbW_{18}O_{60}]^{9-}$ in **1** and sandwich-type $[Ni_4(H_2O)_2(AsW_9O_{34})_2]^{10-}$ in **2**. Both of compounds **1–2** crystallize in a low-symmetrical space group of *P*-1 and consist of a complicated supramolecular network based on non-covalent intermolecular weak interactions, including hydrogen bonding and $\pi\cdots\pi$ stacking. The multipoint hydrogen bonding interactions constitute the structural feature in two supramolecular frameworks. The UV–vis, fluorescence and electrochemistry properties are also studied.

1. Introduction

Polyoxometalate (POM) clusters are of significant contemporary interest owing to their intriguing structures, interesting electrical and optical properties and catalytic activities [1]. As a kind of nano-sized metal oxygen anions, POMs have been employed as important inorganic building blocks to construct novel hybrid materials with various organic molecules [2]. Such compounds not only combine the advantages of inorganic metal-oxo clusters and organic molecules, such as structural fine-tuning, but also the close interaction and synergistic effect of inorganic and organic moieties [3]. One of focuses in this field is to explore novel lattice architectures resulting from the association of organic molecules and POM anions. Therefore, POM chemistry has also become one of many areas in inorganic chemistry that is developing most rapidly [4].

In our ongoing efforts to develop synthetic and functional analogs of POM-based hybrids, our research has focused on the synthesis of POM-based assemblies through non-covalent weak interactions occurred among surface oxygen atoms of POMs and organic molecules [5]. Some supramolecular architecture based on Keggin-, Dawson- and isooctamolybdate-type clusters, assembling with decorated bipyridine cations have been reported [6,7]. In this field, the non-classical polyanions are not paid equivalent attention and still underdeveloped, presumably due to the reasons of the size, charge, and chemical stability [8]. Among them, the $\{M_{18}\}$ (M=Mo or W) cluster cage has many versatile features, such as electronic configurability or use as a synthetic platform, which should allow the design of novel functional nano-objects [9]. Usually, these non-classical polyoxoanions have higher negative charges than classical Keggin and Dawson polyoxoanions [10], they need more organic cations for the balance and may emerge novel structure features [11]. Therefore, we choose the non-classical $[SbW_{18}O_{60}]^{9-}$ and $[Ni_4(H_2O)_2(AsW_9O_{34})_2]^{10-}$ polyoxoanions as candidates for constructing supramolecular assemblies with bipyridine cations. The linear bi-functional 'spacer' or 'rod' trans-1,2-di-(4-pyridyl)-ethylen (bpe) is a particularly good candidate to produce unique structural motifs with beautiful esthetics and useful functional properties owing to its conjugated system [12]. In current work, bpe is explored as organic moiety to assemble non-classical metal-oxo W_{18} anions. Two compounds with formulas: $(H_2bpe)_{3.5}H_2[SbW_{18}O_{60}]\cdot 5H_2O$ (**1**), and $(H_2bpe)_5[Ni_4(AsW_9O_{34})_2(H_2O)_2]\cdot 3H_2O$ (**2**) have been prepared and characterized. Their structural investigating reveals that non-covalent interactions play important roles in the self-organization process of these assemblies. The results further illustrate that polyanions can structure this kind of rigid and conjugated organic molecules into a parallel and ordered arrangement [13]. The UV, fluorescence and CV properties of **1–2** were studied.

2. Experimental section

2.1. Materials and physical measurements

All chemicals purchased were of reagent grade and used without further purification. Elemental analyses were carried on

* Corresponding authors. Fax: +86 311 86269217.
E-mail address: hanzg116@yahoo.com.cn (Z. Han).

0022-4596/$ - see front matter © 2011 Elsevier Inc. All rights reserved.
doi:10.1016/j.jssc.2011.01.041

a Perkin-Elmer 2400 CHN elemental analyzer. FTIR spectra were recorded in the range 400–4000 cm^{-1} on an Alpha Centaurt FTIR spectrophotometer using a KBr pellet. TG analyses were performed on a Perkin-Elmer Pyris Diamond TG/DTA instrument in flowing N_2 with a heating rate of 10 °C min^{-1}. Cyclic voltammograms (CV) were recorded on a 384B polarographic analyzer. A CHI 660 Electrochemical Workstation connected to a Digital-586 personal computer was used for control of the electrochemical measurements and for data collection. A conventional three-electrode system was used. The working electrode was a modified CPE. An Ag/AgCl (saturated KCl) electrode was used as a reference electrode and a Pt gauze as a counter electrode. All potentials were measured and reported versus the Ag/AgCl electrode.

2.2. Preparation

Synthesis of $(H_2bpe)_{3.5}H_2[SbW_{18}O_{60}]\cdot 5H_2O$ (**1**): A mixture of Sb_2O_3 (60 mg, 0.21 mmol), $Na_2WO_4\cdot 2H_2O$ (350 mg, 1.06 mmol), $NiSO_4\cdot 6H_2O$ (40 mg, 0.2 mmol) and bpe (50 mg, 0.25 mmol) was dissolved in 15 mL distilled water at room temperature and stirred for another 3 h. Then, the pH value of the mixture was adjusted to ca. 4 with 4 mol L^{-1} HCl, and stirred for another 1 h. The suspension was put into a Teflon-lined autoclave and kept under autogenous pressure at 170 °C for 6 days. After slow cooling to room temperature, yellow block crystals were filtered and washed with distilled water (32% yield based on W). Anal. Calcd% for $C_{84}H_{106}N_{14}O_{130}Sb_2W_{36}$ (10255.91): C, 9.83; H, 1.01; N, 1.91. Found%: C, 9.63; H, 1.11; N, 2.12. IR (cm^{-1}): 541(w), 765(s), 883(m), 962(s), 2101(w), 1500(m), 1627(m), 1652(m), 3068(m).

Synthesis of $(H_2bpe)_5[Ni_4(AsW_9O_{34})_2(H_2O)_2]\cdot 3H_2O$ (**2**): A mixture of Na_3AsO_4 (200 mg, 0.4 mmol), $Na_2WO_4\cdot 2H_2O$ (350 mg, 1.0 mmol), $NiSO_4\cdot 6H_2O$ (40 mg, 0.2 mmol) , bpe (50 mg, 0.25 mmol) was dissolved in 10 mL distilled water at room temperature and stirred for another 3 h. And then, the pH value of the mixture was adjusted to ca. 6 with 6 mol L^{-1} HCl, and stirred for another 1 h. The suspension was transferred into a Teflon-lined autoclave and kept under autogenous pressure at 150 °C for 10 days. After slow cooling to room temperature, yellow block crystals were filtered and washed with distilled water (39% yield based on W). Anal. Calcd% for $C_{60}H_{70}As_2N_{10}Ni_4O_{73}W_{18}$ (5792.98): C, 12.44; H, 1.19; N,2.42. Found%: C, 12.67; H, 1.28; N, 2.36 . IR (cm^{-1}): 708(m), 761(s), 841(w), 889(s), 945(w), 1128(m), 1152(m), 1627(s), 3421(s).

The IR spectra for **1–2** were placed into Supporting Materials as Fig. S1.

2.3. X-ray crystallography

The data for compounds **1–2** were collected at room temperature with a Bruker Smart Apex CCD diffractometer with Mo$K\alpha$ monochromated radiation (λ=0.71703 Å). Routine Lorentz and polarization corrections were applied. The structures of **1–2** were solved by direct methods and refined by the full-matrix least-squares methods on F^2 using the SHELXTL crystallographic software package [14]. Anisotropic thermal parameters were used to refine all non-hydrogen atoms. Positions of the hydrogen atoms attached to carbon atoms were fixed at their ideal positions. Protonated hydrogen atoms attached to nitrogen atoms were located from the difference Fourier map and were constrained. A summary of the crystallographic data and structural determination for **1–2** is provided in Table 1. The intermolecular hydrogen bond interactions are provided in Table 2. Some typical bond lengths are listed in Table s1. CCDC 786897 and 786898 contain the supplementary crystallographic data for **1** and **2**, respectively. These data can be obtained free of charge via http://www.ccdc.cam.ac.uk/conts/retrieving.html, or from the Cambridge Crystallographic Data Centre, 12 Union Road, Cambridge CB2 1EZ, UK; fax: (+44) 1223-336-033; or e-mail: deposit@ccdc.cam.ac.uk.

Table 1
Crystal data and structure refinement for **1–2**.

Compound reference	**1**	**2**
Chemical formula	$C_{84}H_{104}N_{14}O_{130}Sb_2W_{36}$	$C_{60}H_{70}As_2N_{10}Ni_4O_{73}W_{18}$
Formula mass	10251.91	5792.98
Crystal system	Triclinic	Triclinic
a/Å	13.408(4)	15.5969(10)
b/Å	13.913(4)	17.8244(11)
c/Å	25.689(8)	20.5325(13)
α/°	91.795(5)	67.7400(10)
β/°	102.529(4)	89.9150(10)
γ/°	114.456(4)	85.9170(10)
Unit cell volume/Å^3	4219(2)	5267.3(6)
Dc/mg cm^{-3}	4.035	3.653
Space group	$P\bar{1}$	$P\bar{1}$
Z	1	2
Reflections measured	20865	27436
Independent reflections	14484	18269
R_{int}	0.0425	0.0346
R_1 values ($I>2\sigma(I)$)	0.0848	0.0627
$wR(F^2)$ values ($I>2\sigma(I)$)	0.2474	0.1705
R_1 values (all data)	0.1118	0.0926
$wR(F^2)$ values (all data)	0.2697	0.2051
Goodness of fit on F^2	1.045	1.003

2.4. Preparation of compounds *1–2* modified carbon paste electrodes (CPEs)

0.5 g graphite powder and 0.05 g compound **1** (or **2**) were mixed, and ground together by agate mortar and pestle to achieve an even, dry mixture; to the mixture 0.50 mL paraffin oil was added under stirring with a glass rod; then the mixture was packed into 3 mm inner diameter glass tube, and the surface was pressed tightly onto weighing paper with a copper rod through the back. Electrical contact was established with copper rod through the back of the electrode.

3. Results and discussion

3.1. Synthesis and structure

The crystal structure analyses revealed that two compounds are formed from organic bpe cation and different polytungstate anions: pseudo-Dawson $[SbW_{18}O_{60}]^{9-}$ in **1** and sandwich-type $[Ni_4(H_2O)_2(AsW_9O_{34})_2]^{10-}$ in **2** (see Scheme 1). Both of the compounds were obtained by using simple oxide and inorganic salts as raw materials to fabricate big anionic clusters under hydrothermal conditions. During the reiterated experiments, it was found that the central heteroatoms play a crucial role in isolating the targeted anionic clusters. Under the same reaction conditions, replacing Sb with P, Si led to the Keggin-type anions. The presence of a lone electron pair of the center heteroatom Sb^{3+} which has a larger ionic radius prevents the formation of the sandwich-type M_4-POMs. In **1**, the Sb^{3+} is surrounded pyramidally by three oxygen atoms, and the lone pair orbital electrons are located on the top of the pyramid. In **2**, the central As^{5+} atoms are a tetrahedral coordination-geometry. In addition, the pH values of reaction solutions also play important role in assembling process of anionic clusters. The results showed that the higher pH value (ca. 6) is good for isolation sandwich-type anion. Though the raw material $NiSO_4$ does not existed in the crystal **1**, the reiterative

Table 2
Intermolecular hydrogen bonding interactions in compounds **1-2**.

D–H…A	D–H(Å)	H…A(Å)	D…A(Å)	D–H…A(°)
Compound **1**				
N(1)–H(1B)…O(20^{i})	0.87	2.27	3.03(5)	151
N(2)–H(2B)…O(48^{ii})	0.86	1.98	2.76(5)	151
N(4)–H(4B)…O(55)	0.86	2.27	3.10(5)	163
N(5)–H(5A)…O(29^{iii})	0.86	2.43	3.25(5)	158
N(6)–H(6B)…O(64)	0.86	1.90	2.74(5)	166
N(7)–H(7B)…O(62^{iv})	0.86	1.98	2.82(6)	161
O(63)–H(63A)…O(36)	0.90	2.13	2.96(4)	154
O(64)–H(64A)…O(59^{v})	0.90	2.10	2.97(5)	162
O(65)–H(65A)…O(58^{vi})	0.85	2.04	2.83(4)	154
C(4)–H(4A)…O(21^{iii})	0.93	2.58	3.48(5)	164
C(16)–H(16A)…O(11^{ii})	0.93	2.40	3.33(6)	175
C(21)–H(21A)…O(10^{ii})	0.93	2.36	3.25(5)	160
C(26)–H(26A)…O(31^{vii})	0.93	2.20	3.08(5)	156
C(29)–H(29A)…O(58^{iii})	0.93	2.57	3.43(5)	154
Symmetry code: *i*=2–*x*,2–*y*,1–*z*; *ii*=−1+*x*,*y*,*z*; *iii*=1–*x*,1–*y*,1–*z*; *iv*=1+*x*,1+*y*,*z*; *v*=1–*x*,−*y*,1–*z*; *vi*=*x*,1+*y*,*z*; *vii*=*x*,*y*,1+*z*				
Compound **2**				
N(1)–H(1B)…O(47^{i})	0.86	1.84	2.69(2)	166
N(2)–H(2B)…O(40^{iii})	0.86	2.06	2.78(3)	140
N(3)–H(3A)…O(31)	0.86	1.95	2.78(2)	163
N(4)–H(4B)…O(32^{iv})	0.86	2.03	2.81(3)	150
N(5)–H(5B)…O(25)	0.86	2.26	2.97(2)	140
N(6)–H(6B)…O(43^{v})	0.86	2.23	2.97(3)	144
N(7)–H(7B)…O(3W^{vi})	0.86	1.68	2.45(2)	149
Nv9)–H(9B)…O(5^{vi})	0.86	2.10	2.92(2)	157
N(10)–H(10B)…O(26^{v})	0.86	1.90	2.757(17)	172
O(1W)–H(1WB)…O(24^{ii})	0.85	2.30	3.07(2)	151
C(1)–H(1A)…O(44^{i})	0.93	2.36	3.28(2)	169
C(2)–H(2A)…O(30^{vii})	0.93	2.39	3.30(2)	166
C(11)–H(11A)…O(42^{iii})	0.93	2.19	3.04(3)	150
C(16)–H(16A)…O(59^{vi})	0.93	2.36	3.26(2)	162
C(17)–H(17A)…O(16)	0.93	2.29	3.21(2)	170
C(23)–H(23A)…O(51^{vi})	0.93	2.40	3.27(3)	156
C(28)–H(28A)…O(52)	0.93	2.44	3.29(3)	153
C(41)–H(41A)…O(13^{vi})	0.93	2.47	3.31(2)	151
C(48)–H(48A)…O(14^{vi})	0.93	2.39	3.16(3)	140
Symmetry code: i=1–*x*,2–*y*,–*z*; *ii*=1–*x*,1–*y*,–*z*; *iii*=1+*x*,–1+*y*,*z*; *iv*=1–*x*,–*y*,1–*z*; *v*=–*x*,1–*y*,1–*z*; *vi*=1–*x*,1–*y*,1–*z*; *vii*=1+*x*,*y*,*z*				

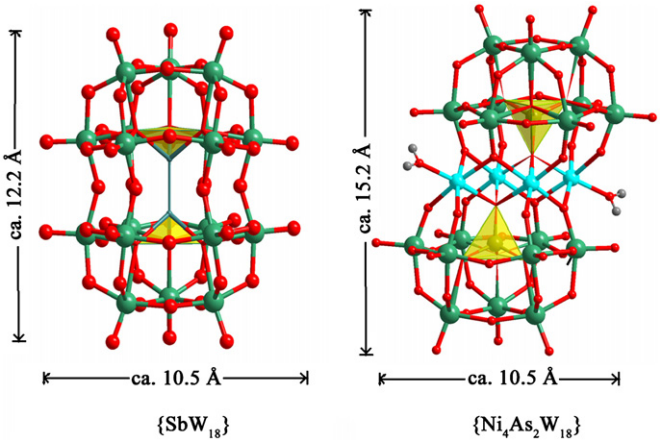

Scheme 1. Views showing the structures of inorganic W_{18} anions.

experiments showed that it is indispensable for the successful isolation of **1**, which may play a role of auxiliaries.

Bond valence sum calculations [15] for compounds **1–2** show that all W atoms are in the +6 oxidation state and Sb atom is in the +3 oxidation state, and Ni atoms are in the +2 oxidation state; As atoms are in +5, respectively. Additionally, the assignment of the oxidation state is also consistent with the coordination geometry of atoms.

Compound 1: Single-crystal X-ray diffraction analysis shows that the structural unit of **1** is constructed from one pseudo-Dawson-like polyoxoanion $[H_2SbW_{18}O_{60}]^{7-}$ anion, three and a half H_2bpe cations and five lattice water molecules (Fig. 1). The analogous Dawson-like anion $[H_2SbW_{18}O_{60}]^{7-}$ was originally presented by Krebs and Klein [16]. The polyoxoanion $[SbW_{18}O_{60}]^{9-}$ represents an antimony-containing Dawson-like polyoxotungstate approaching the D_{3h} point symmetry, and contains two B-α-$[Sb_{0.5}W_9O_{33}]^{12.5-}$ moieties linked together through corner-sharing connection by elimination of six oxygen atoms. Here, the presence of a lone electron pair of the center heteroatom Sb^{3+} prevents the formation of the classical Dawson-type cluster and prefers to adopt $[SbW_{18}O_{60}]^{9-}$. Only one {Sb} group distributes two central positions of two $\{W_9\}$ entities with fractional occupancy (0.5) (Sb···Sb=2.171(6) Å). The Sb^{3+} is surrounded pyramidally by three oxygen atoms, and the lone pair orbital electrons are located on the top of the pyramid. The Sb-O bond distances are 1.98(2)–2.03(2) Å with a mean value of 2.010 Å. There are alternating "short" and "long" W–O_b–W bonds owing to small displacement of W atoms from the mirror planes of the W_3O_{13} triplets. These W–O bond distances can be classified into usual three groups: (i) W–O_t(terminal), 1.64(3)–1.77(3) Å; (ii) W–$O_{\mu 2}$(bridge), 1.83(2)–1.98(2) Å; (iii) W–$O_{\mu 4}$(central), 2.17(2)–2.32(2) Å, respectively.

Intermolecular hydrogen bonding and π stacking interactions are the most important and also extensive synthons in fabricating a supramolecular framework. In the structure of **1**, owing to the conjugated π-electron system of bpe, the organic moiety exhibits regular packing with face-to-face π···π interactions among adjacent molecules, leading to an interesting organic angle-rule arrangement. The near distances fill into the range of 3.294–3.419 Å, indicating more strong π···π interactions. There

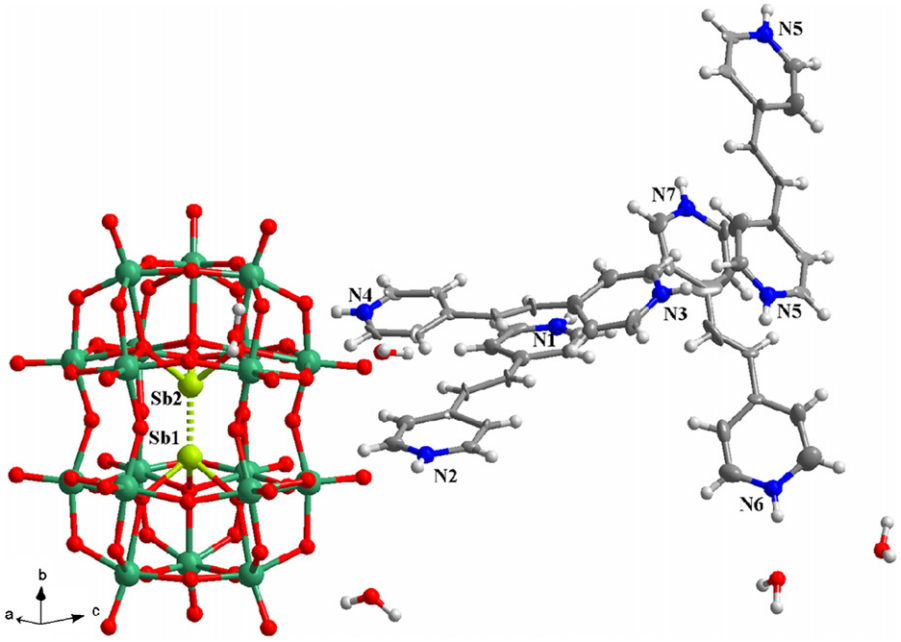

Fig. 1. ORTEP drawing with thermal ellipsoids at 50% probability showing the basical unit in **1**.

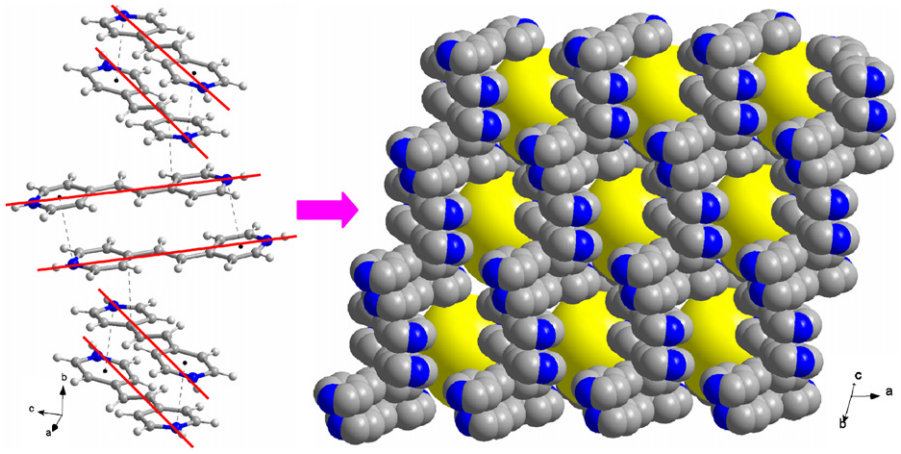

Fig. 2. View showing the interesting organic angle-rule arrangement of bpe and space-filling view showing the self-assembly of inorganic and organic moieties in **1**. Yellow ball anion. (For interpretation of the references to colour in this figure legend, the reader is referred to the web version of this article.)

are four crystallographically distinct bpe molecules that are labeled as N(1)-bpe, N(3)-bpe, N(5)-bpe and N(7)-bpe, respectively, in which the N(5)-bpe molecule lies at an invert center of (1,1,1). As shown in Fig. 2, two parallel N(1)-bpes and two parallel N(3)-bpes together make two components of the organic angle-rule, respectively. The corner between two components is ca. 59.7° angle. There are extensive and effective intermolecular N–H···O and C–H···O interactions among/between organic cations and inorganic anions (Table 2). These intermolecular interactions direct the ordered assembly of inorganic and organic moieties (Fig. S2). Fig. 3 represents the layer-like space-filling view seen along the *a* axis, indicating that the inorganic and organic moieties stack alternatively.

Compound 2: The composition of **2** consists of sandwich-type $[Ni_4(H_2O)_2(AsW_9O_{34})_2]^{10-}$ anions and bi-protonated bpe cations (see Fig. 4). The polyoxoanion $[Ni_4(OH_2)_2(AsW_9O_{34})_2]^{10-}$ may be seen as two tri-lacunary $[B\text{-}\alpha\text{-}(AsW_9O_{34})_2]^{9-}$ fragments of Keggin units linked by four edge-linked $\{NiO_6\}$ octahedra with coplanar nickel atoms, leading to a sandwich-type structure with idealized C_{2v} symmetry. The $[B\text{-}\alpha\text{-}(AsW_9O_{34})_2]^{9-}$ comes from the saturated Keggin unit $[AsW_{12}O_{40}]^{3-}$ by removing three adjacent edge-sharing $\{WO_6\}$ octahedra. There are four crystallographically unique Ni(II) ions in the compound **2**. All of Ni(II) centers are octahedrally coordinated pattern with the Ni–O distances of 1.967(12)–2.121(11) Å. However, the coordination environments for them are different: Ni(1) and Ni(4) are coordinated by six oxygen atoms coming from two different $[B\text{-}\alpha\text{-}(AsW_9O_{34})_2]^{9-}$ units; Ni(2) and Ni(3) are coordinated by five oxygen atoms belong to two different $[B\text{-}\alpha\text{-}(AsW_9O_{34})_2]^{9-}$ units and one water molecule. The central belt of anion is four coplanar $\{NiO_6\}$ octahedral sharing edges to form a rhombic $\{Ni_4O_{16}\}$ groups (see Fig. S3). The distances are Ni(1)···Ni(2)=3.196 Å, Ni(1)···Ni(2i)=3.185 Å, Ni(1)···Ni(1i)=3.275 Å, Ni(2)···Ni(2i)=5.476 Å (i: $1-x$, $1-y$, $-z$); Ni(3)···Ni(4ii)=3.185 Å, Ni(3)···Ni(4)=3.193 Å, Ni(4)···Ni(4ii)=3.266 Å, Ni(3)···Ni(3ii)=5.479 Å(ii: $-x$, $1-y$, $1-z$), and the angles are Ni(1)···Ni(2)···Ni(1i)=61.78°, Ni(2)···Ni(1)···Ni(2i)=118.22°, Ni(4)···Ni(3)···Ni(4i)=61.60° and Ni(3)···Ni(4)···Ni(3i)=118.40°, respectively. These values for the metal–metal separation and the geometry of the bridging unit are similar to the first example of sandwich-type

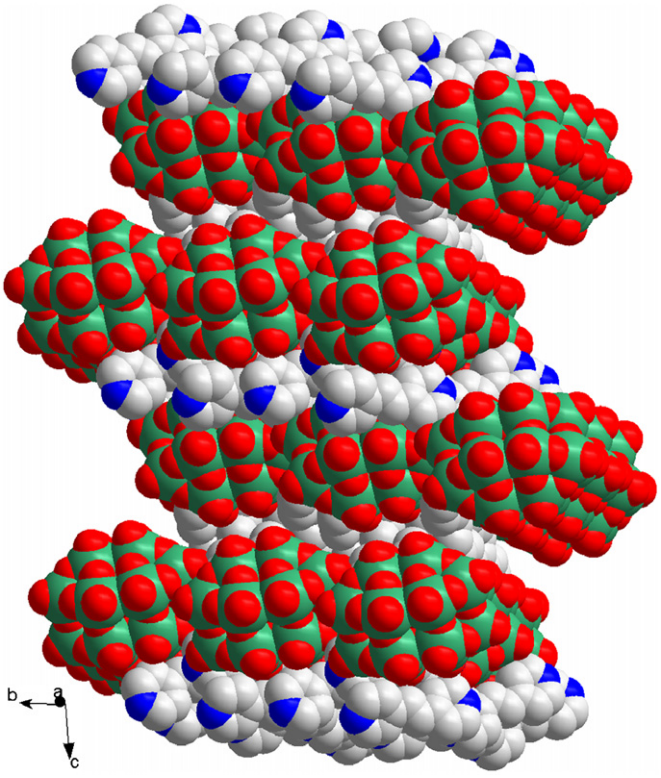

Fig. 3. Space-filling view showing the layer-like arrangement of **1** in *bc* plane.

phosphorus-containing polyanion $[Co_4(OH_2)_2(PW_9O_{34})_2]^{10-}$ reported by Weakley et al. [17].

There are five kinds of cystallographically distinct bpe cations as the 'spacers' to link sandwich-type anions into a complicated supramolecular framework. Beside the π stacking interactions, interestingly, there is plenty of multipoint hydrogen bonding interactions in **2** (see Fig. S4). As shown in Fig. 5, a structural feature of **2** is that the rod-shaped N(5)- and N(8)-containing bpes like arrows point to the windows formed by $\{W_4O_4\}$ groups. The distances between the protonated N atoms and the bridging μ_2-O atoms are N(5)···O=2.853∼3.060 Å and N(8)···O=2.894–2.963 Å, indicating weak multipoint hydrogen bond interactions. Thus, an interesting organic bi-capped sandwich-type structure is presented, which we reported recently while using organic molecules to assemble Keggin-type anions [5b,6b,18]. So, the 'spacer' bpe cations bridge anionic clusters into a chain array. Distances involving N–H···O–W, and C–H···O–W weak interactions are shown in Table 2. The 'inclusion' packing mode of compound **2** illustrates that the polyanions play a template-agent role in inducing the self-assembly process of organic cations via its surface oxygen involved into the directional hydrogen bonds (see Fig. 6).

Both of compounds **1–2** crystallize in a low-symmetrical space group of *P*-1 and consist of a complicated supramolecular framework based on non-covalent intermolecular weak interactions. A simple comparison between **1** and **2** shows that there is more regular face-to-face π···π interactions in the supramolecular framework of compound **1** than that in **2**; more multipoint hydrogen bonding interactions in **2** than that in **1**. The mechanism of the formation of different assemblies is yet to be understood.

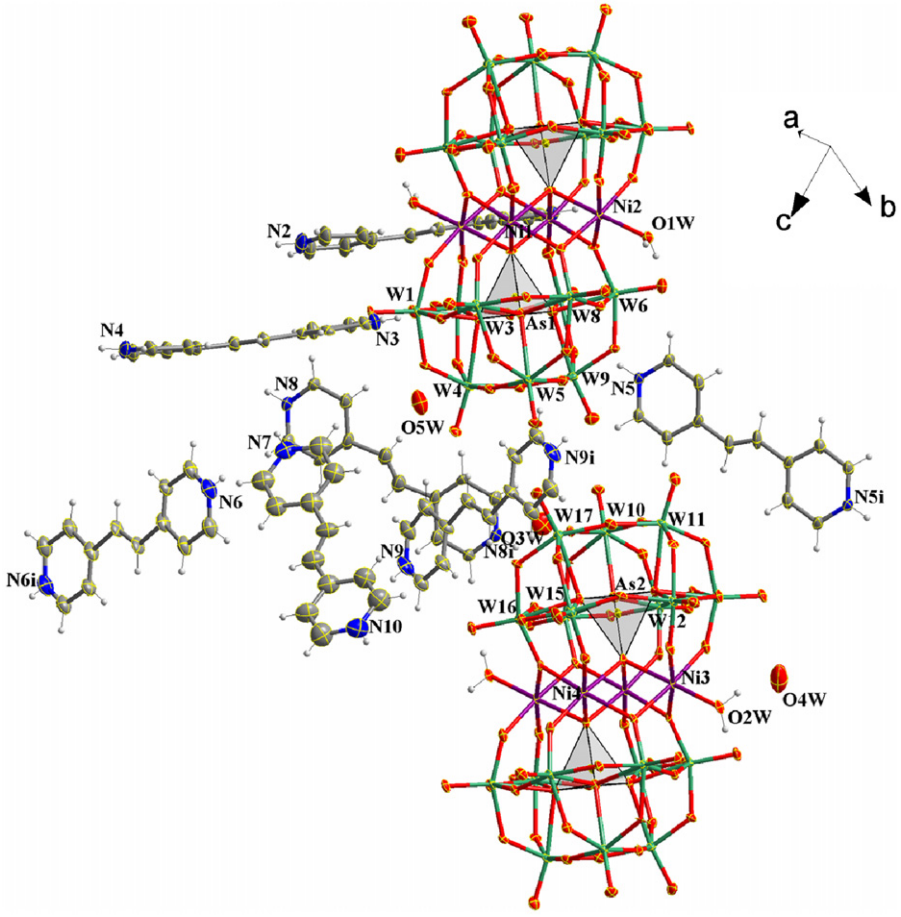

Fig. 4. ORTEP drawing of **2** showing the labels of atoms with thermal ellipsoids at 30% probability.

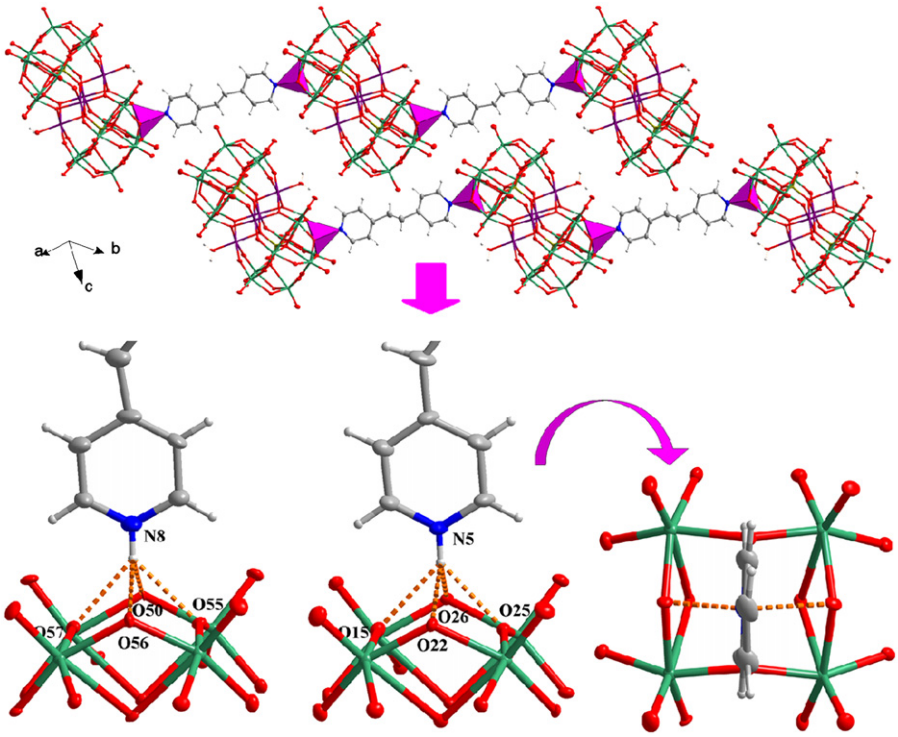

Fig. 5. Ball-and-stick views showing the hybrid chain containing organic bi-capped-cluster units based on the multipoint hydrogen bonding interaction between sandwich anions and bpe cations in **2**. The distances are N(5)···O=2.853~3.060 Å and N(8)···O=2.894~2.963 Å.

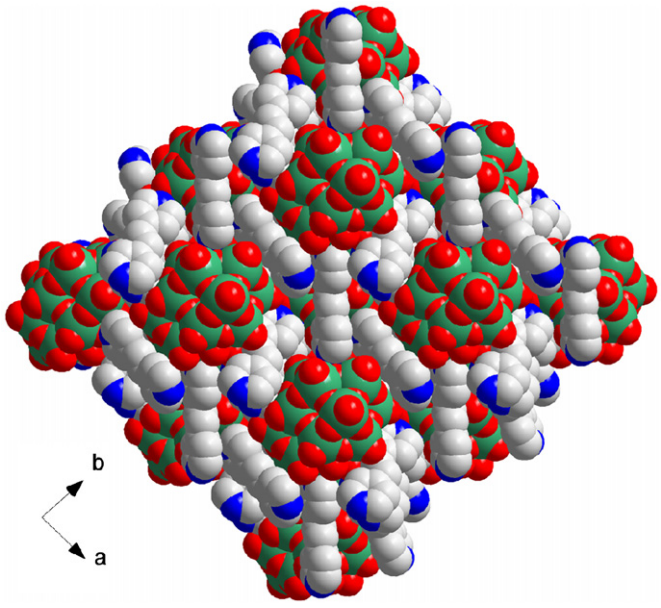

Fig. 6. Space-filling view showing the 'inclusion' assembly in **2**.

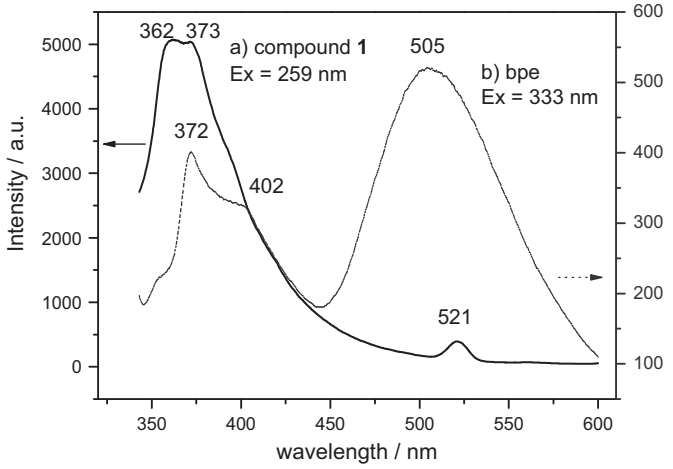

Fig. 7. The fluorescence curves of **1** and free bpe in CH_3OH.

However, it appears that the appropriate combination of starting materials, size and ratio of anion and cation, acidity, and hydrothermal synthetic conditions can lead to the formation of POM-based supramolecular structures with different geometrical and structural characteristics.

3.2. *UV–vis and fluorescence measurement*

The UV spectra (Fig. s5) of the solutions of bpe, **1** and **2** soaked in CH_3OH were measured respectively. Peaks at 208 and 285 nm for **1** and 207 and 287, 298 nm for **2** in the UV–vis region are observed, which are assigned to the charge-transfer absorption band of terminal and bridging oxygen atoms to metal centers (208 nm for **1** and 207 nm for **2**), and the π electrons transitions of organic bpe cations (285 nm for **1** and 287, 298 nm for **2**). Because of the conjugated π electron system of bpe, the fluorescence spectra of **1–2** had also been studied. The fluorescence emission at 362, 373 and 521 nm of **1** occurs as a result of excitation at 259 nm (see Fig. 7); the peaks at 321, 358 and 515 nm of **2** excited at 256 nm (see Fig. S6). Excitation of free bpe at λ=333 nm produces luminescence with the peak values at 372, 402 and 505 nm, respectively. These UV and fluorescence data indicated that compounds may be entirely disruptive in dilute solution, which was also observed in previous papers too [19]. However, the changes in peaks' position and intensity suggest that, within the solution, the absorption interaction should at least occur among bpe cations and polyanions. The origin of the emission

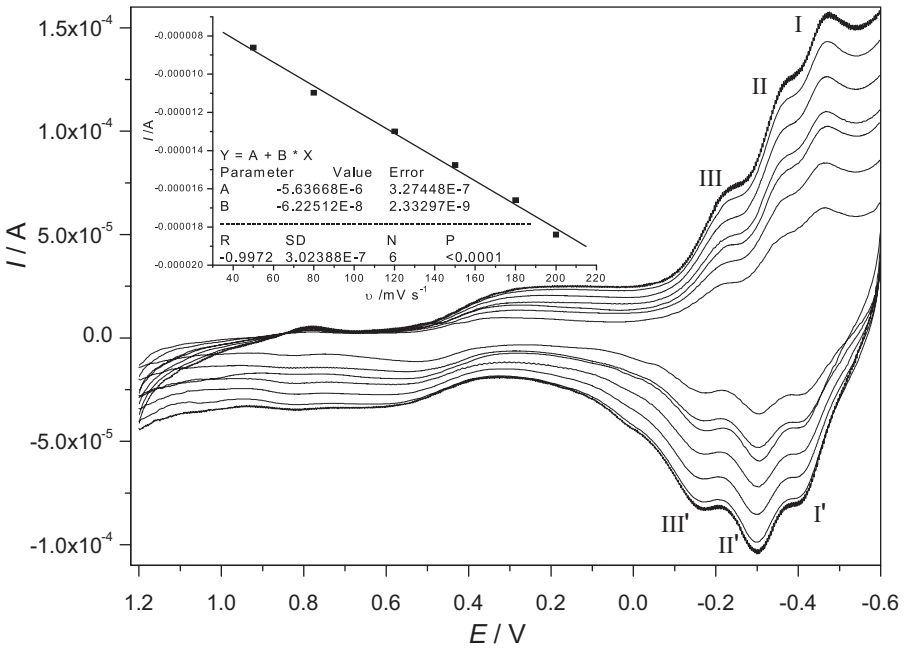

Fig. 8. The redox properties of compound **1**-CPE were studied in 1 M H_2SO_4 aqueous solution at the different scan rates. Scan rates (from inner to outer): 50, 80, 100, 120, 150, 180, 200 mV s^{-1}. The inset figure represents the currents of peaks II' against scan rates.

for compounds **1** and **2** can be tentatively attributable to $\pi^* \rightarrow \pi$ transitions of bpe.

3.3. Voltammetric behavior and thermogravimatric analysis

The redox properties of **1–2** (CPE) were studied in 1M H_2SO_4 aqueous solution at the different scan rates and are shown in Fig. 8 and Fig. S7, respectively. For **1**-CPE, there are three pairs of redox peaks for W atoms in the range from −0.6 to 0.2 V. The oxidation peaks with the values of −0.467, −0.352 and −0.373 V and two reduction peaks with the potentials of −0.408, −0.308 and −0.223 V at a scan rate 50 mV s^{-1}, respectively. The $E_{1/2}=(E_{pa}+E_{pc})/2$ are −437 mV (I), −330 mV (II) and −298 mV(III). Redox peaks I–I′, II–II′ and III–III′ should be ascribed to three consecutive two-electron processes of W, respectively [20]. When the scan rate varied from 50 to 200 mV s^{-1}, the peak potentials changed gradually: the cathodic peak potentials shifted toward the negative direction and the corresponding anodic peak potentials to the positive direction with increasing scan rates varied from 50 to 200 mV s^{-1}. The inset figures show that the peak II′ currents are proportional to the scan rates, indicating that the redox process of **1**-CPE is surface-controlled. For **2**-CPE, two pairs of the redox peaks are observed in the range from −0.8 to 0.2 V. The $E_{1/2}$ values are −653 mV(I) and −483(II) (scan rate: 100 mV s^{-1}). The different redox behaviors may be originated from the effect of polyanions and the organic-inorganic hybrid framework in **1–2** [21].

The thermal gravimetric (TG) analysis was performed with N_2 atmosphere at 20–800 °C for the compounds. The TG curves (see Fig. S8) of two compounds indicate a three-stage process of weight loss in the measuring temperature range. The loss of crystal waters was finished until 180 °C, followed by a continuous two-step weight loss of bpe in two compounds. The weight loss process was completely finished until 710 °C in **1** and 820 °C in **2**. The whole weight losses (27.3% and 26.3%) are consistent with the calculated value (27.1% and 27.5%) for **1** and **2**, respectively, corresponding to the decomposition of crystal water molecules and bpe ligands.

4. Conclusions

Two supramolecular assemblies built upon W_{18}-oxygen clusters and the rigid rod-like bpe cations are reported. The results illustrate that polyanions can structure this kind of rigid and conjugated organic molecules into a parallel and ordered arrangement. Current results suggest that self-processes are actively involved in the ways that individuals (inorganic clusters and organic rigid molecules) respond to their roles to control the formation of multidimensional inorganic–organic networks. Studies in this respect are going on to reveal the synthetic rules and to explore their attractive properties.

Acknowledgments

This work was financially supported by the Natural Science Foundation of China (20701011), and Doctoral Initial Foundation of Hebei Normal University (L2005B13), and the Education Department Foundation of Hebei Province (Z2006436).

Appendix A. Supporting information

Supplementary data associated with this article can be found in the online version at doi:10.1016/j.jssc.2011.01.041.

References

[1] (a) H.N. Miras, G.J.T. Cooper, D.L. Long, H. Bögge, A. Müller, C. Streb, L. Cronin, Science 327 (2010) 72–74;
(b) P.P. Mishra, J. Pigga, T.B. Liu, J. Am. Chem. Soc. 130 (2008) 1548–1549;
(c) Q.S. Yin, J.M. Tan, C. Besson, Y.V. Geletii, D.G. Musaev, A.E. Kuznetsov, Z. Luo, K.I. Hardcastle, C.L. Hill, Science 328 (2010) 342–345;
(d) G.G. Gao, P.S. Cheng, T.C.W. Mak, J. Am. Chem. Soc. 131 (2009) 18257–18259.
[2] (a) H.Y. An, E.B. Wang, D.R. Xiao, Y.G. Li, Z.M. Su, L. Xu, Angew. Chem. Int. Ed. Engl. 45 (2006) 904–908;
(b) J.Y. Niu, P.T. Ma, H.Y. Niu, J. Li, J.W. Zhao, Y. Song, J.P. Wang, Chem. Eur. J. 13 (2007) 8739–8748;
(c) X.L. Wang, Y.F. Bi, B.K. Chen, H.Y. Lin, G.C. Liu, Inorg. Chem. 47 (2008) 2442–2448;

(d) J.W. Zhao, H.P. Jia, J. Zhang, S.T. Zheng, G.Y. Yang, Chem. Eur. J. 13 (2007) 10030–10045;
(e) S.T. Zheng, J. Zhang, G.Y. Yang, Angew. Chem. Int. Ed. Engl. 47 (2008) 3909–3913;
(f) Y.Q. Lan, S.L. Li, X.L. Wang, K.Z. Shao, D.Y. Du, H.Y. Zang, Z.M. Su, Inorg. Chem. 47 (2008) 8179;
(g) Z.G. Han, T. Chai, X.L. Zhai, J.Y. Wang, C.W. Hu, Solid State Sci. 11 (2009) 1998–2002.
[3] (a) E. Coronado, J.R. Galán-Mascarós, C. Giménez-Saiz, C.J. Gómez-García, E. Martínez-Ferrero, M. Almeida, E.B. Lopes, S.C. Capelli, R.M. Llusar, J. Mater. Chem. 14 (2004) 1867–1872;
(b) E. Coronado, C. Giménez-Saiz, C.J. Gómez-García, S.C. Capelli, Angew. Chem., Int. Ed. 43 (2004) 3022–3025;
(c) Y.F. Song, D.L. Long, L. Cronin, Angew. Chem. Int. Ed. 46 (2007) 3900–3904.
[4] (a) D.L. Long, E. Burkholder, L. Cronin, Chem. Soc. Rev. 36 (2007) 105–121;
(b) T.B. Liu, E. Diemann, H.L. Li, A.W.M. Dress, A. Müller, Nature 426 (2003) 59–61;
(c) C.P. Pradeep, D.L. Long, G.N. Newton, Y.F. Song, L. Cronin, Angew. Chem. Int. Ed. 47 (2008) 4388–4391;
(d) D.L. Long, L. Cronin, Chem. Eur. J. 12 (2006) 3698–3706.
[5] (a) Z.G. Han, Y.L. Zhao, J. Peng, H.Y. Ma, Q. Liu, E.B. Wang, N.H. Hu, H.Q. Jia, Eur. J. Inorg. Chem. 2 (2005) 264–271;
(b) Z.G. Han, Y.L. Zhao, J. Peng, A.X. Tian, Q. Liu, J.F. Ma, E.B. Wang, N.H. Hu, CrystEngComm 7 (2005) 380–387;
(c) A.X. Tian, J. Ying, J. Peng, J.Q. Sha, Z.G. Han, J.F. Ma, Z.M. Su, N.H. Hu, H.Q. Jia, Inorg. Chem. 47 (2008) 3274–3283.
[6] (a) Z.G. Han, Y.L. Zhao, J. Peng, A.X. Tian, Y.H. Feng, Q. Liu, J. Solid State Chem. 178 (2005) 1386–1394;
(b) Z.G. Han, Y.L. Zhao, J. Peng, H.Y. Ma, Q. Liu, E.B. Wang, N.H. Hu, J. Solid State Chem. 177 (2004) 4325–4331;
(c) Z.G. Han, Y.L. Zhao, J. Peng, H.Y. Ma, Q. Liu, E.B. Wang, J. Mol. Struct. 738 (2005) 1–7;
(d) A.X. Tian, Z.G. Han, J. Peng, J.L. Zhai, Y.L. Zhao, Z. Anorg. Allg. Chem. 633 (2007) 495–503.
[7] Z.G. Han, Y.G. Gao, C.W. Hu, Cryst. Growth Des. 8 (2008) 1261–1264.
[8] (a) J.P. Wang, P.T. Ma, J.Y. Niu, Sci. China Ser. B—Chem. 50 (2007) 784–789;
(b) D.L. Long, P. Kögerler, L. Cronin, Angew. Chem. Int. Ed. 43 (2004) 1817–1820.
[9] J. Yan, D.L. Long, E.F. Wilson, L. Cronin, Angew Chem. Int. Ed. 121 (2009) 4440–4444.
[10] B. Krebs, R. Klein, in: M.T. Pope, A. Müller (Eds.), Polyoxometalates: From Platonic Solids to Anti-Retroviral Activity, Kluwer Academic Publishers, Dordrecht, 1994, p. 41.
[11] (a) D.L. Long, C. Streb, Y.F. Son, S. Mitchell, L. Cronin, J. Am. Chem. Soc. 130 (2008) 1830;
(b) J.P. Wang, P.T. Ma, J.W. Zhao, J.Y. Niu, Inorg. Chem. Commun. 10 (2007) 523.
[12] X.J. Li, R. Cao, D.F. Sun, W.H. Bi, Y.Q. Wang, X. Li, M.C. Hong, Cryst. Growth Des. 4 (2004) 775–780.
[13] Z.G. Han, Y.G. Gao, X.L. Zhai, J. Peng, A.X. Tian, Y.L. Zhao, C.W. Hu, Cryst. Growth Des. 9 (2009) 1225–1234.
[14] (a) G.M. Sheldrick, SHELXS-97, Program for Crystal Structure Solution, University of Göttingen, Göttingen (Germany), 1997;
G.M. Sheldrick, SHELXL-97, Program for Crystal Structure Refinement, University of Göttingen, Göttingen, Germany, 1997.
[15] I.D. Brown, D. Alternatt, Acta Cryst. B 41 (1985) 244–247.
[16] (a) B. Krebs, R. Klein, in: M.T. Pope, A. Müller (Eds.), Polyoxometalates: From Platonic Solids to Anti-Retroviral Activity, Kluwer Academic Publishers, Dordrecht, 1994, p. 55.
[17] T.J.R. Weakley, H.T. Evans, J.S. Showell, G.F. Tourné, C.M. Tourné, J. Chem. Soc. Chem. Commun. (1973) 139.
[18] Z.G. Han, T. Chai, Y.N. Wang, Y.Z. Gao, C.W. Hu, Polyhedron 29 (2010) 196–203.
[19] (a) J.Y. Niu, X.Z. You, C.Y. Duan, H.K. Fun, Z.Y. Zhou, Inorg. Chem. 35 (1996) 4211–4217;
(b) J.Y. Niu, Q. Wu, J.P. Wang, J. Chem. Soc. Dalton Trans. (2002) 2512–2516.
[20] (a) Z.G. Han, Y.L. Zhao, J. Peng, Q. Liu, E.B. Wang, Electrachim. Acta 51 (2005) 218–224;
(b) J. Canny, F.X. Liu, G. Hervé, C. R. Chimie 8 (2005) 1011–1016;
(c) N. Fay, E. Dempsey, T. McCormac, J. Electroanal. Chem. 574 (2005) 359–366;
(d) W. Zhang, S.X. Liu, P. Sun, C.D. Zhang, F.J. Ma, D. Feng, J. Mol. Struct. 968 (2010) 76–80.
[21] I.M. Mbomekalle, B. Keita, Y.W. Lu, L. Nadjo, R. Contant, N. Belai, M.T. Pope, Eur. J. Inorg. Chem. (2004) 276.